

# Threshold production of charmed and B mesons in $e^+e^-$ annihilation \*

Nina Byers

*Physics Department, UCLA, Los Angeles, CA 90024*

(December 9, 1994)

## Abstract

After an historical introduction reviewing the successes and failures for heavy quarkonium spectroscopy of the nonrelativistic quark model including  $(v/c)^2$  corrections, the discussion is widened to include light quark pair creation; i.e., dynamical quarks. We find that the simple extension of the QCD inspired potential model which includes dynamical quarks first proposed by Eichten et al. [2] is remarkably successful in accounting both for the observed narrow state heavy quarkonium spectroscopy *and* experimental data on threshold production of charmed and B mesons in  $e^+e^-$  annihilation. We have studied various different models of light quark pair creation. In addition to the original Cornell model, we find that a variant of it can also account for the data. The cross section data are mainly inclusive cross section measurements. The two models give distinguishably different predictions for the energy dependence of production cross sections for individual channels, and measurement of the

---

\*Presented at the International Conference on QUARK CONFINEMENT AND THE HADRON SPECTRUM, Villa Olmo – Como, Italy, 20-24 June 1994. To be published in the Proceedings of the Conference.

energy dependence of production cross sections for individual channels may distinguish between these models.

## I. INTRODUCTION

In this talk I would like to discuss three sorts of QCD inspired phenomenological models which describe  $Q\bar{Q}$  physics at low energies. [1] The simplest is the nonrelativistic naive quark model (NR NQM). By naive quark model (NQM), I refer to treatments in which the problem is treated strictly as a two body problem. As I remind you below, the NR NQM initially had many successes. However, there were also some failures which were put right when  $(v/c)^2$  corrections were taken into account. I will discuss separately two types of  $(v/c)^2$  corrections; (i) those applied to the NQM and (ii) extension of the NQM to take into account light quark pair creation. This is one of the two main points of my talk, namely that light quark pair creation effects are  $(v/c)^2$  corrections to the NQM and are of the same order as effects due to the spin dependence of the  $Q\bar{Q}$  force and kinematic  $(v/c)^2$  corrections. All these effects are important in obtaining good agreement of quark model predictions with experimental data. There are two types of light quark pair creation effects to be discussed here; namely, (1) those that occur in heavy quarkonium states below flavor threshold (vacuum polarization effects) and (2) those responsible for production of charmed and B mesons at low energies. The effects of virtual light quark pairs on the narrow  $Q\bar{Q}$  states below flavor threshold can be included through modification of the two-body  $Q\bar{Q}$  potential. If one confines one's attention only to these states, then the phenomenological  $Q\bar{Q}$  potential obtained by fits to data includes both the two-body potential and the effect on the spectrum of virtual  $q\bar{q}$  pairs. Such a treatment, however, does not allow for relating the effects of virtual  $q\bar{q}$  pair creation with actual  $q\bar{q}$  pair creation as seen in the productions of charmed and B mesons. It is also somewhat inadequate in that it is difficult to obtain the configuration mixing necessary to account for certain spectroscopic results without explicit inclusion of four-body  $Q\bar{q}q\bar{Q}$  virtual states.

In section II is a brief summary of the successes, and failures, of the NR NQM; and, in section III, the improvement when  $(v/c)^2$  corrections and the spin-dependence of the  $Q\bar{Q}$  interaction are taken into account. Section IV presents some QCD inspired potential models of light quark pair creation. Section V outlines the method used to include these dynamical quarks in calculating both the spectroscopy of the narrow  $Q\bar{Q}$  states below flavor threshold and the production cross sections for charmed and B mesons above flavor threshold. Of the various possible models we studied in detail, two seem reasonably successful in accounting for both the observed spectroscopy of the narrow states and the observed threshold production cross sections in  $e^+e^-$  annihilation. These models are the Cornell model [2] and an extension of it studied by Zambetakis [5]. Section VI compares predictions of these models with available production cross section data. These are mainly inclusive cross section data. Both models give remarkably good accounts of these data but neither are precise fits to the data. This section also presents exclusive production cross sections; for these the models predict different energy dependences. Measurement of exclusive production cross sections may indicate which of these models is the more correct one.

## **II. SUCCESSES AND FAILURES OF THE NONRELATIVISTIC NAIVE QUARK MODEL (NR NQM).**

This section is something of an historical account which is incomplete and included here to give background to the assertion that corrections to the NR NQM owing to light quark pair creation, and the coupled channel mixing it induces, are of the same order as those due to spin-dependent forces and other  $(v/c)^2$  corrections.

### **A. Successes**

Here are outlined the early outstanding successes of the NR NQM. Using a simple QCD inspired potential which behaves at short distances like a one gluon exchange potential and is linearly rising at large distances, the model has as parameters the strength of the Coulombic

part and the slope of the linear part of the potential; in addition, the masses of the c and b quarks. With these few parameters, the model accounts quite well for a large number of data:

Masses of narrow heavy quarkonium states (spin averaged).

Leptonic decay rate ratios  $\Gamma_{ee}(\psi')/\Gamma_{ee}(\psi)$ , etc..

Allowed radiative transition rates (given by  $\langle r \rangle_{fi}$ ); e.g.,  $\psi' \rightarrow \chi_J$ ,  $\chi_J \rightarrow J/\psi$ , etc..

Allowed M1 radiative transition rates (given by  $\langle 1 \rangle_{fi}$ ); e.g.,  $J/\psi \rightarrow \eta_c$ .

### B. Failures

Among the successes above were some failures. These were:

$\Gamma_{ee}(J/\psi)$  too big.

E1 radiative transition rate for  $\psi' \rightarrow \chi_0$  too big by a factor 2.

Forbidden M1 transitions such as  $\psi' \rightarrow \eta_c$  observed.

$\psi(3770)$  observed in  $e^+e^-$  annihilation with mass too close to the  $\psi'$  to be understandable as a  $^3S_1 c\bar{c}$  state.

In addition this simple model failed to account for the observed fine and hyperfine splittings in the spectra. The items above, and the fine structure of the mass spectra, are corrected by taking relativistic corrections into account.

### III. RELATIVISTIC CORRECTIONS.

There are two types of relativistic corrections: (i)  $(v/c)^2$  corrections to the NQM; i.e.,  $(v/c)^2$  corrections to the nonrelativistic potential model in which nevertheless the model remains a two-body treatment of the problem, and (ii) extension of the model to take into

account dynamical quarks; i.e., light quark pair production. Type (i) relativistic corrections have been discussed in this Conference explicitly by G. M. Prosperi, Yu-Bing Dong, L. Fulcher, F. Schoeberl, H. Sazdjian, Kuan-Ta Chao, and extensively in the literature; see, e.g., [7,8] and references cited therein. Spin-dependent forces are also regarded as type (i)  $(v/c)^2$  corrections because they arise in this order in the Breit-Fermi reduction of a particle exchange diagram. Estimates of the spin-dependence of the  $Q\bar{Q}$  force have been obtained other ways as well; see, e.g., [3,4] and the contributions of J. M. Ball and F. Zachariasen to this Conference. The effects that I would classify as type (ii) relativistic corrections are those that arise owing to virtual light quark pairs. These are of the same magnitude as those of type (i) and arise in relativistic quantum field theory in order  $(v/c)^2$ . Below is a list of relativistic corrections which have been found to correct the 'failures' mentioned above. In most cases several effects contribute.

- a. spin-orbit  $Q\bar{Q}$  interaction
- b. spin-spin  $Q\bar{Q}$  interaction
- c. tensor forces
- d. spin-independent  $(v/c)^2$  corrections to the  $Q\bar{Q}$  Hamiltonian
- e. direct  $Q\bar{Q}$   $^3D_1$  - photon coupling
- f. light quark pair creation
- g. coupled channel mixing.

In Table I. are indicated which of the above items tend to correct the so-called failures.

put right	by
Fine structure splitting	a
E1 rate $\psi' \rightarrow \chi_0$	a and g
$\Gamma_{ee}(J/\psi)$	g
Forbidden M1 rates	d and g
$\psi(3770)$ explained	c, e, and g
$\sigma(e^+e^- \rightarrow \text{charmed mesons})$	f

**Table I.**

I have not included hyperfine splittings in the above discussion. This is because I believe that remains an unsolved problem.

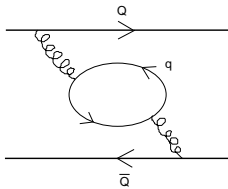
The bulk of this paper is about light quark pair creation. The foregoing was included to indicate that inclusion of light quark pair creation improves the the agreement of NQM results with experimental data in two ways. Not only does it extend the model to describe quarkonium decays to charmed and B mesons, it also improves the agreement with the narrow state spectroscopic data.

Before addressing explicitly light quark pair creation effects, it is appropriate here to remind you that relativistic effects such as spin-orbit couplings, as well as pair creation, reflect the Lorentz transformation properties of the interaction. For example, in a Breit-Fermi Hamiltonian the spin-orbit interaction coming from vector and scalar exchange have opposite sign and differ by a factor 3. Correspondingly pairs created from vector and scalar exchange are produced in  $1^{--}$  and  $0^{++}$  states, respectively. At present it is not clear that the spin-orbit interaction is correctly viewed as an effect found in a Breit-Fermi reduction of vector and scalar exchange interactions. However, when this assumption is made and the result compared with data the observed fine structure splittings indicate that the long range (linearly rising) part of the potential comes from scalar exchange. We included light quark pair creation in such a model and found this coupling to decay channels incapacitated the model. (See below.) On the other hand, models in which the quarkonium potential

as a whole is assumed vector exchange can account well for the (spin-averaged) masses [5]; ‘vector’ models also account reasonably well for observed threshold charmed and B meson production cross section data. Therefore, it may be reasonable to assume there is some truth in these ‘vector’ models. They are not inconsistent with the analyses of Eichten and Feinberg [3] and Gromes [4] who obtain in a  $1/M^2$  expansion of QCD spin-dependent  $Q\bar{Q}$  interactions similar to those obtained in the Breit-Fermi reduction of a vector short range and scalar long range potential.

#### IV. INCLUDING DYNAMICAL QUARKS

Eichten et al. proposed a quarkonium potential model that includes dynamical quarks nearly 20 years ago. [2] Their framework, with various different dynamical assumptions, has been used by most authors writing on this subject since then. Straightforward inclusion of light quark pair creation in a  $Q\bar{Q}$  model requires quantum field theory and immediately confronts us with a many body problem to solve. Eichten et al., hereafter referred to as the Cornell group, simplified the problem to manageable proportions. Before going into details about model predictions for charmed and B meson productions, I would like to briefly outline their framework. Its structure incorporates fundamental properties of QCD, namely confinement and asymptotic freedom. Consider the QCD vacuum polarization diagram shown below.



For loop momenta large compared to constituent quark masses, this diagram can be treated perturbatively and is taken into account using the QCD running coupling constant. However, diagrams with small loop momenta should be treated nonperturbatively. For low momenta, higher order diagrams with multiple gluon exchanges should be taken into account. These

were included by the Cornell group invoking duality. They used a phenomenological field theoretic model for  $q\bar{q}$  creation and then took the strong interactions into account by replacing the  $Q\bar{q}q\bar{Q}$  intermediate states by  $Q\bar{q}$  and  $q\bar{Q}$  mesons (bound by the same potential as binds  $Q\bar{Q}$ ). This reduces the many body problem to a tractable pair of two-body problems.

First one solves a potential model for bound  $Q\bar{Q}$ ,  $Q\bar{q}$  and  $q\bar{Q}$  states. The Cornell group used

$$V(r) = -\frac{\kappa}{r} + C + \frac{r}{a^2} . \quad (1)$$

Then, as in the Wigner-Weisskopf treatment of coupled channel problems in nuclear physics, one solves a coupled channel two-body problem that can be represented by the Hamiltonian

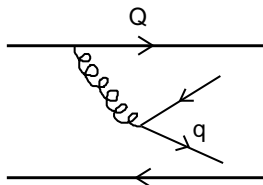
$$H = \begin{pmatrix} H_{Q\bar{Q}} & h^\dagger \\ h & H_{Q\bar{q}q\bar{Q}} \end{pmatrix} \quad (2)$$

which operates in a space of bound  $Q\bar{Q}$  states and bound  $Q\bar{q}$  and  $q\bar{Q}$  states. In the Cornell model the  $Q\bar{Q}$  states are eigenstates of

$$H_{Q\bar{Q}} = \frac{p^2}{M_Q} + V + 2M_Q . \quad (3)$$

and the  $Q\bar{q}$  and  $q\bar{Q}$  mesons eigenstates of the corresponding Hamiltonian (with relativistic correction for the light quark). In the calculations, however, measured (or to be measured) values of the  $Q\bar{q}$  and  $q\bar{Q}$  meson masses are used. The piece denoted by  $H_{Q\bar{q}q\bar{Q}}$  in (2) is the kinetic energy operator for the two-meson states. The off-diagonal piece  $h$  couples the  $Q\bar{Q}$  states to their two-body decay channels. (Final state interactions are neglected; i.e., interactions between the bound  $Q\bar{q}$  and  $q\bar{Q}$  mesons are neglected.)

To complete the framework described above, we need to put in a mechanism for pair creation. In the Cornell model, pairs are created by the same interaction that binds; i.e., by diagrams such as





where the corkscrew line represents the propagator of an (instantaneous) interaction whose Fourier transform is the quarkonium potential  $V$ . The quark vertices, correspondingly, were taken as nonrelativistic reduction of a vector exchange. One may vary these assumptions and consider other dynamical models of quark pair creation. For example, one could assume scalar rather than vector exchange. As mentioned above, the fine structure in the mass spectra indicate that the long distance part of the potential may be due to scalar exchange. These two assumptions give quite different results; a vector interaction creates a pair with quantum numbers  $1^{--}$  while a scalar creates a pair with the quantum numbers of the vacuum. We can report here calculations based upon various different assumptions about the dynamics of  $q\bar{q}$  pair production. They are tabulated in Table II.


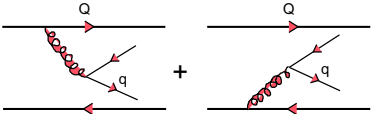
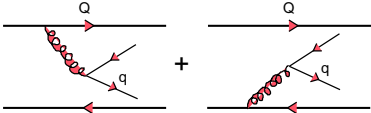
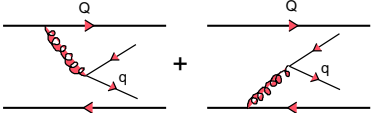
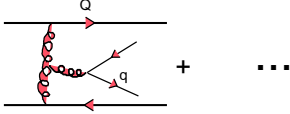
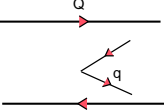
Model	$h$		ex
<b>Cornell</b>		$r/a^2$	V
<b>Zambetakis</b>		$V(r)$	V
<b>Grotch, Zamb, Byers</b>		$-\kappa/a + fC$ $+ (1-f)C + r/a^2$ $\{0 \leq f \leq 1\}$	V S
<b>Grotch &amp; Byers</b>		order $\alpha_s^2$ QCD	V
<b>Le Yaouanc et al., ...</b>		$\frac{m_q \gamma_{QPC}}{\sqrt{2}}$	S

Table II.

The dynamical assumptions represented in Table II. are as follows. First, the Cornell model: the original Cornell model neglected pair creation from the Coulombic part of the

potential and took pair creation only from the long distance part. This is indicated in the third column. In the fourth column is indicated whether the exchange is vector or scalar. The second row represents Zambetakis' extension of the original Cornell model to include the Coulombic part of the potential in the pair creation matrix elements. [5] The third row represents our calculations with Howard Grotch in which we took the Coulombic part of the potential to be vector exchange and the long range part to be scalar. There is an ambiguity in implementing this idea; namely where does short become long? Quantitatively this translates into the question of how to treat the constant term  $C$  in (1). For vector coupling,  $C$  plays no role; the pair creation matrix elements only depend on the gradient of the potential. However with scalar coupling the potential behaves like a mass term and the pair creation matrix elements depend on  $V$  rather than  $\vec{\nabla}V$ . Thus the constant  $C$  can be significant. Fits to the data indicate  $C$  is large and negative; of the order of  $-800$  MeV. [5] To take this ambiguity into account, we introduced another parameter  $f$  which specifies which fraction of  $C$  couples vectorially, and allowed it to vary between 0 and 1. The fourth row refers to calculations with Grotch of the contribution of the triple gluon coupling graph. We evaluated this graph in Coulomb gauge, and found its contributions were not large; they are indeed of order  $\alpha_s^2$ . We also studied the other QCD graphs of this order and found none seems to be singular. We therefore conclude that such effects are not at this stage significant. In the last row is represented the QPC model of Le Yaouanc et al.. [12] It is a model sometimes referred to as a flux tube or string breaking model. In it the  $q\bar{q}$  are produced with the quantum numbers of the vacuum, and the pair creation matrix element is a constant which can be included in calculations like the above by taking it to be given by a constant potential  $m_q\gamma_{QPC}/\sqrt{2}$ . This model gives interesting results which have been discussed in a number of papers; see Ref. [12].

In order to get the matrix elements of  $h$  from the diagrams in Table II., one must sandwich them between  $Q\bar{Q}$  wave functions and  $Q\bar{q}$  and  $q\bar{Q}$ . (Generally the  $Q\bar{Q}$  wave functions are taken to be eigenstates of (3), and for simplicity the  $Q\bar{q}$  and  $q\bar{Q}$  wave functions are taken to be Gaussian fits to bound state wave functions bound by the  $r/a^2$  part of the potential.)

We report here the results of our studies of first four of these models. Mainly what we have to report are our results for the Cornell and Zambetakis models because (1) we found the order  $\alpha_s^2$  graphs were not likely to be large enough to be important; (2) the hybrid model in which the long range part of the potential was considered scalar exchange was unsuccessful (explained below); and (3) both the Cornell and Zambetakis models were able to account for available data - a large amount of data on the narrow states below threshold and on production cross sections for charmed and B mesons above threshold. This is will be discussed in detail in the last section of this paper.

We end this section with a brief explanation of why we think that the hybrid model of short distance vector and long distance scalar exchange is not a viable model. Allowing  $f$  to vary between 0 and 1, we could not find values of the parameters in the potential (1) that allowed a fit to the narrow state spectroscopic data. The reason for this is that in the region of  $r$  where the quarkonium wave functions are large  $V$  changes sign, going from Coulombic at short distances to linearly rising at large distances, and consequently, when it is coupled as a scalar, its contributions to matrix elements of  $h$  are relatively small differences of two large numbers. Owing to this the matrix elements of  $h$  vary erratically as one goes from one of the low-lying quarkonium states to another; consequently their contributions to level shifts are unstable against small variations of the parameters.

## V. MODIFICATION OF NQM

Before discussing our numerical results, it may be of interest to outline here how the inclusion of dynamical quarks changes the NQM. This can best be seen in a Hamiltonian framework in which the light quarks have been integrated out and one has remaining an effective Hamiltonian in the  $Q\bar{Q}$  space. This is a peculiar Hamiltonian because (i) it is energy-dependent; and (ii) for energies above threshold for meson production, it develops an anti-hermitian part. It is, however, quite interesting because it gives mass shifts and configuration mixings and also gives production cross sections for charmed and B mesons in

$e^+e^-$  annihilation.

In the space spanned by eigenstates of (3), hereafter called NQM states, the effective Hamiltonian is (see, e.g., Refs. [5,9])

$$H_{eff}(W) = \mathcal{M}^{bare} + \Omega(W) . \quad (4)$$

where  $\mathcal{M}^{bare}$  is a diagonal matrix whose elements are the eigenvalues of (3). The  $\Omega$  matrix is second order in  $h$ ; the explicit expression for it is given below. It is perhaps useful to state some more of the properties of  $H_{eff}$  here.

(1). The physical masses  $M_N$  of the narrow quarkonium states are given by the solutions to

$$H_{eff}(M_N) a^N = M_N a^N \quad (5)$$

where  $a^N$  denotes a state vector in the space spanned by NQM states. A physical state  $\Psi_N$  may be expanded as

$$\Psi_N = \sum_i a_i^N \psi_i + \sum_n b_n^N \phi_n . \quad (6)$$

where  $\psi_i$  are NQM states and  $\phi_n$  are continuum two-meson states. The  $a_i^N$  are the components of the ‘eigenvectors’  $a^N$  in (5). The problem (5) is not exactly an eigenvalue problem. The dependence on  $M_N$  is highly nonlinear. Nevertheless solutions can be found. [5]

(2).  $H_{eff}(W)$  is not hermitian when  $W$  is above the threshold of the lowest mass two-meson continuum. The quarkonium states whose masses are above threshold are poles in the complex  $W$  plane. They are poles of the effective propagator  $\mathcal{G}(W)$ , where

$$\mathcal{G}(W) = (W - H_{eff}(W))^{-1} . \quad (7)$$

For  $W$  above threshold,  $\Omega$  has the structure

$$\Omega(W) = R(W) - i\Gamma(W)/2 \quad (8)$$

with  $R$  and  $\Gamma$  real symmetric matrices. Unitarity requires the diagonal elements of  $\Gamma$  to be positive.

The matrix elements of  $\Omega(W)$  are given by

$$\Omega_{ji}(W) = \sum_n \frac{(\psi_j, h^\dagger \phi_n)(\phi_n, h\psi_i)}{(W - E_n + i\epsilon)}. \quad (9)$$

The sum over  $n$  denotes sum over channels and integration over channel phase space;  $E_n$  is the channel energy. The channels are labeled by  $f$  which specifies channel spins, flavor, masses, etc.. Because of this sum over channels,  $\Omega$  is a sum of matrices

$$\Omega(W) = \sum_f \Omega^{(f)}(W). \quad (10)$$

Each matrix element of  $\Omega^{(f)}$  is an integral which becomes singular when  $W \geq m_1 + m_2$  where  $m_1$  and  $m_2$  are the masses of the mesons in channel  $f$ . These singular integrals are evaluated in the usual way taking  $W$  in the upper half plane and then the boundary value on the real axis from above.

For  $W$  above flavor threshold, charmed and B meson production cross sections in  $e^+e^-$  annihilation may be calculated as follows. The cross section ratio

$$\Delta R^f = \frac{\sigma(e^+e^- \rightarrow f)}{\sigma(e^+e^- \rightarrow \mu^+\mu^-)}, \quad (11)$$

in one photon approximation, is given by the dispersive part of  $\mathcal{G}(W)$ . With a high speed computer and  $H_{eff}$  in matrix form (see below),  $\mathcal{G}$  is easily calculated by matrix inversion. There is no coupling between the  $c\bar{c}$  and  $b\bar{b}$  subspaces, so one deals separately with these two subspaces and the calculations for the production cross sections of charmed and B mesons are done independently. The charm contribution to the cross section ratio  $\Delta R_c$  can be expressed as a trace in the  $c\bar{c}$  subspace; viz.,

$$\Delta R_c = -\frac{72\pi}{W^2} e_c^2 \mathbf{Tr}(\mathcal{W} \frac{(\mathcal{G} - \mathcal{G}^\dagger)}{2i})_{c\bar{c}} \quad (12)$$

where  $e_c = 2/3$ , and the matrix  $e_c^2 \mathcal{W}$  is bilinear in the  $c\bar{c}$ -photon coupling. Nonrelativistically, matrix elements of  $\mathcal{W}$  are given by  $c\bar{c}$  NQM wave functions; viz.,

$$\mathcal{W}_{ij} = \psi_i(0)\psi_j(0). \quad (13)$$

(Relativistic corrections are important here, particularly for charm; see Ref. [10].) In their original papers, the Cornell group showed that

$$\mathcal{G} - \mathcal{G}^\dagger = \mathcal{G}^\dagger(\Omega - \Omega^\dagger)\mathcal{G}. \quad (14)$$

Thus, from (12), (14), and (10), one sees that the exclusive production cross section for channel  $f$  is

$$\Delta R_c^{(f)} = -\frac{72\pi}{W^2} e_c^2 \mathbf{Tr}(\mathcal{W} \mathcal{G}^\dagger \text{Im}\Omega^{(f)} \mathcal{G})_{c\bar{c}}. \quad (15)$$

Similarly, one calculates production cross sections for B mesons. From the above it is clear that this is a nonperturbative treatment of dynamical quarks.

With high speed computers it is straightforward to solve, as outlined above, for both the narrow states below threshold and the (resonant) cross sections above threshold. One first solves (3) for the NQM wave functions and masses. The matrix elements of the  $\Omega$  matrix and (4) can then be explicitly evaluated. These matrix elements are discrete because, owing to confinement, the entire  $Q\bar{Q}$  state space is spanned by a discrete set of eigenfunctions. With these matrices one can calculate all of the above quantities. Most computers are now able to work with matrices of (almost) arbitrarily high dimension. However, since we are interested only in the low lying quarkonium states, we do not need to calculate matrices of high dimension. The highly excited NQM states make negligible contributions.

On the other hand, another approximation involved in a numerical evaluation of  $\Omega(W)$  may cause significant error in predicted masses of quarkonium resonances in the continuum. In calculating  $\Omega(W)$  one generally approximates the infinite sum over channels  $f$  by a finite sum neglecting all channels with thresholds greater than some minimum energy  $E_{min}$

which is greater than the maximum value of  $W$  for which one is calculating the  $\Omega$  matrix. Though the contribution from any one of these neglected channels is small, their cumulative effect can be appreciable because all these channels contribute coherently (negatively) to the diagonal elements of  $\text{Re } \Omega$ ; c.f., Eq. (9). (Cancellations are likely in contributions to the off-diagonal elements owing to random phases.) These cumulative mass shifts are small for  $W$  substantially below  $E_{min}$ ; however, they may become appreciable when  $W$  comes close to  $E_{min}$ .<sup>1</sup>

## VI. PRODUCTION CROSS SECTION CALCULATIONS AND COMPARISON WITH EXPERIMENTAL DATA

In this section we report our results on threshold production cross sections, inclusive and exclusive, for charmed and B mesons in  $e^+e^-$  annihilation and compare them with available data. There are two sets of results; one obtained from the original Cornell model and the other from Zambetakis' extension in which pair creation occurs at short distances also. The available data are mainly inclusive cross section measurements. The agreement with data is about the same for both although it differs in detail in the two cases. The two models give significantly different results for exclusive channel cross sections. Measurement of these may distinguish between them. The degree of agreement of these model predictions with data is, in our view, significant because the calculated cross sections are obtained without adjustment of parameters or introduction of additional parameters. The parameters are the parameters of the potential  $\kappa$ ,  $C$ , and  $1/a^2$ . We calculated the masses of the narrow

---

<sup>1</sup>In our calculations we included only the channels with ground state pseudoscalar and vector mesons. This is a good approximation for the narrow states below flavor threshold; however, for values of  $W$  in the continuum we found it necessary, as did the Cornell group, to compensate for the neglect of excited meson decay channels by putting in a phenomenological mass shift to fit the observed resonance energies [2,11].

charmonium states using (5) and determined these three parameters by fitting the observed masses of  $J/\psi$ ,  $\chi_{c0g}$ , and  $\psi'$ .<sup>2</sup> Parameter values which fit these data are<sup>3</sup>

model	$1/a^2$ in $\text{GeV}^2$	$C$ in $\text{GeV}$	$\kappa(c\bar{c})$
Zambetakis	0.31	-0.97	0.49
Cornell	0.22	-0.85	0.52

Using these parameters, we calculated (spin averaged)  $\Upsilon$  masses, charmonium and  $\Upsilon$  leptonic widths, etc. and found good agreement with measured values [5].<sup>4</sup> Then we calculated charmed and B meson production cross sections above flavor threshold evaluating (15) with the same parameters. We calculated charmed meson production from threshold to 4.5 GeV, and for B from threshold to 11.1 GeV. In the numerical calculations we truncated the  $c\bar{c}$  state space after the 4S and 2D NQM states, as in the original Cornell calculations. We found that including more states did not significantly alter the results. For B meson production, the  $\Upsilon(4S)$  is the first  $b\bar{b}$  resonance above threshold; we truncated after the 7S and 4D NQM states. Results were stable against increasing the number of such states. However, we also found that the results changed little when we omitted the D-states and only changed noticeably near 11 GeV when we omitted the 7S state. The results presented here were

---

<sup>2</sup>After a detailed and extensive analysis, the Cornell group used the following constituent quark masses  $M_c = 1.84$  GeV,  $M_b = 5.17$  GeV, and for light quarks,  $m_u = m_d = 335$  MeV, and  $m_s = 450$  MeV. We used the same values in our calculations.

<sup>3</sup>The slope of the linear potential  $1/a^2$  is significantly greater in Zambetakis' model because the short distance pair creation increases the coupling of  $c\bar{c}$  to inelastic channels. This stronger coupling to inelastic channels increases the separation of charmonium energy levels, and requires increased strength of the confining potential to bring the mass differences back to their observed values.

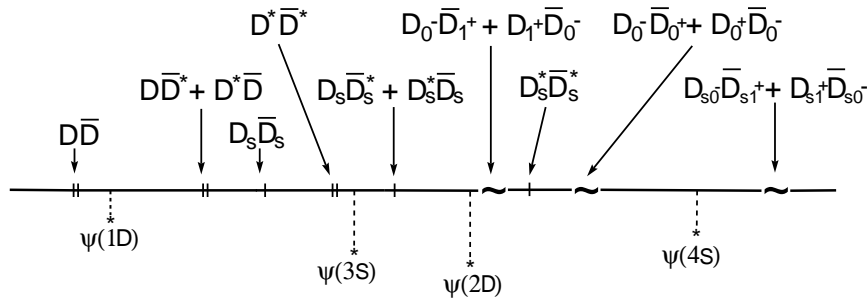
<sup>4</sup>For the  $\Upsilon$  masses and widths, and for B meson production cross sections, the QCD logarithmic decrease of  $\alpha_s$  was taken into account by using for  $\kappa(b\bar{b})$  the values 0.46 and 0.48 for the Zambetakis and Cornell models, respectively.



obtained truncating  $b\bar{b}$  states at the 6S. The reason it was not necessary to include D-states is that owing to the heavier b quark mass, the S-D mixing and photon-D state coupling are smaller than in the charm case.

### A. Charmed meson production.

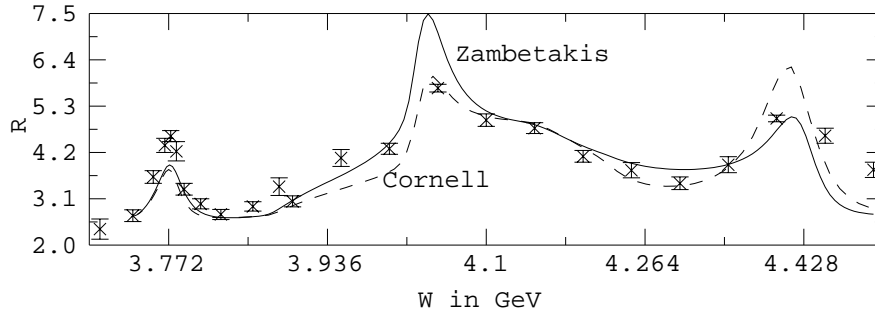
To understand the complicated energy dependence of the inclusive charm production cross section above threshold (3.73 GeV), it is useful to consider the singularities of the  $1^{--} c\bar{c}$  propagator  $\mathcal{G}_{c\bar{c}}(W)$  in the complex energy plane;  $\mathcal{G}(W)$  is given by (7). The singularities are cuts along the real axis and poles in the lower half plane. There is a cut for each open channel with a branch point at its threshold. The poles correspond to resonances in the cross section. The branch points and poles are shown in Fig. 1 where the positions of the singularities are determined by the experimental values of the masses and widths of the indicated states [13]; the distance below the real axis of each pole is the measured total half-width. The separations of the branch points and positions of the poles are to scale.



**Figure 1.**

The corresponding cross section measurements and theoretical curves for R are shown in Fig. 2. The first resonance above threshold is understood, from the point of view of the Cornell model, as the  $\psi(1D)$  though it is not a pure state but has admixtures of other nearby  $1^{--}$  S and D states. Though this is a relatively narrow resonance as indicated by its proximity to the real axis in Fig. 1, it is not as prominent as the S-state peaks,  $\psi(4040)$  and  $\psi(4415)$ , owing to the fact that nonrelativistically D states do not couple directly to the photon. As

it is primarily a D-state, the  $\psi(3770)$  owes its presence in an  $e^+e^-$  annihilation cross section to the fact that it has some configuration mixing with nearby S states ( particularly the 2S) and a direct coupling to the photon in order a  $(v/c)^2$ . Similarly the  $\psi(2D)$  appears in the cross section as a shoulder on the  $\psi(3S)$  or  $\psi(4040)$  peak owing to its admixture of 3S-state and direct coupling to photon.



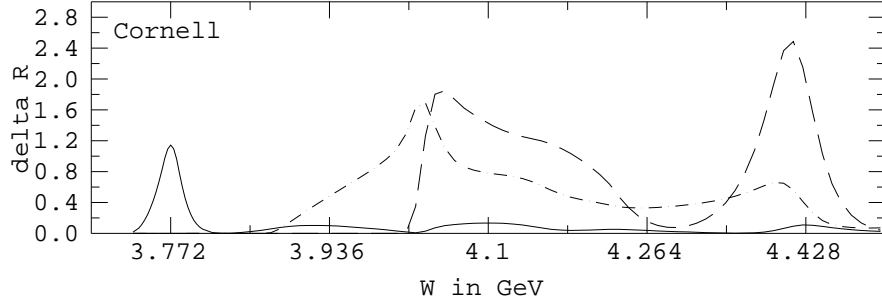
**Figure 2.**

The data points in Fig. 2 are from the *Review of Particle Properties*. [13] The curves are calculated using the Zambetakis and Cornell models with the contribution to  $R$  from other than charmed hadrons taken from the data to be 2.65; i.e., the curves in Fig. 2 are  $\Delta R_c(W) + 2.65$ .<sup>5</sup> What is remarkable about these models is the degree to which the energy dependence and overall normalization of the calculated curves are in agreement with the data. Neither model gives a perfect fit to the data; but considering the simplicity of the models, and the complexity of the physics, it seems remarkable that the models fit the data as well as they do. The Cornell model seems to fit the data in the region of the  $\psi(4040)$  better and the Zambetakis model seems to do better in the region of the  $\psi(4415)$ . It is difficult on the basis of these inclusive cross section data to say if one or the other of these models is closer to being correct.

---

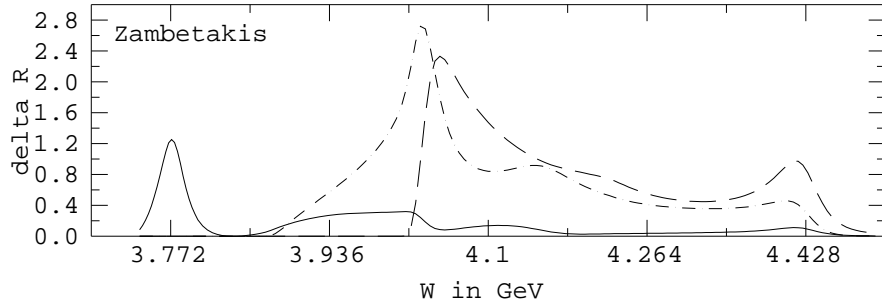
<sup>5</sup> A phenomenological mass shift matrix was used as compensation for the neglect of excited meson decay channels; we only included the ground state pseudoscalar and vector meson decay channels in our calculations, c.f., section V.

The models are more easily distinguished in their predictions for the exclusive cross sections. In Figs. 3 and 4 are shown the individual channel contributions to  $\Delta R_c$ .



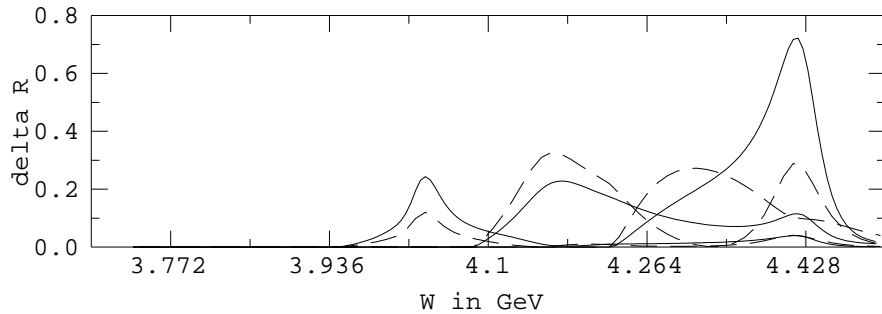
**Figure 3.**

The full curve is the contribution to  $R_c$  from  $D\bar{D}$  channels, both charged and neutral; the dot-dashed curve from  $D\bar{D}^* + D^*\bar{D}$ ; and the dashed curve from  $D^*\bar{D}^*$ .



**Figure 4.**

The cross sections for  $D_s$  and  $D_s^*$  production are roughly 1/3 of those for non-strange D mesons. These are shown in Fig. 5.

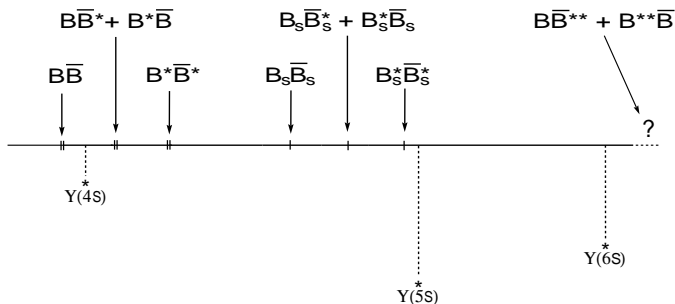


**Figure 5.**

In Fig. 5 the full curves are Cornell model predictions for  $D_s\bar{D}_s$ ,  $D_s\bar{D}_s^* + D_s^*\bar{D}_s$ ,  $D_s^*\bar{D}_s^*$ , and the dashed curves Zambetakis model predictions. The curves for the different channels can be distinguished by the fact that they start at different thresholds. Note the scale change. This suppression of the strange mesons is natural to these models. It comes from the  $m_s$  being greater than  $m_u$ . The suppression is due, essentially, to two effects: (i) the pair creation amplitude is inversely proportional to the light quark mass, and (ii) the strange quark meson states are smaller (more tightly bound).

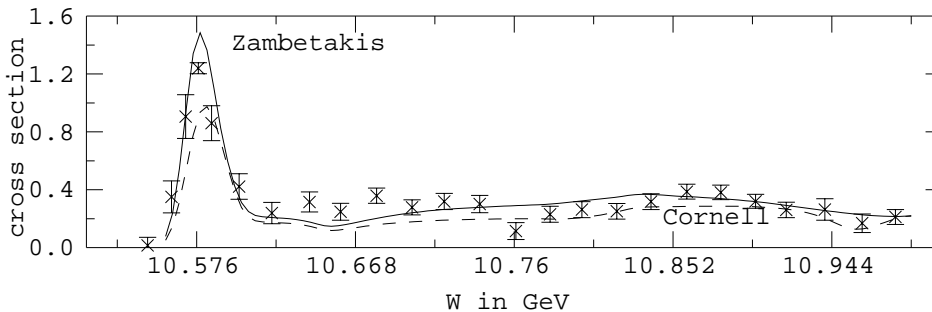
### B. B meson production cross sections.

The singularity structure of  $\mathcal{G}(W)_{b\bar{b}}$  relevant for our purpose is shown in Fig. 6. It appears simpler than Fig. 1 because the  $B^* - B$  mass difference is smaller than  $D^* - D$  and because we have indicated only the S-state resonances. In the  $\Upsilon$  system both S-D mixing and direct photon-D-state coupling are small. These are effects of order  $(v/c)^2$  and therefore smaller than in charmonium. Consequently D-state contributions are not significant in  $e^+e^-$  annihilation cross sections.



**Figure 6.**

Corresponding to this in Fig. 7, we show the inclusive B meson production cross section data [14] along with the calculated curves.



**Figure 7.**

Radiative and beam spreading corrections have been applied to the theoretical curves in Fig. 7 so that they can be compared with the data which are uncorrected for radiative corrections and beam spread.<sup>6</sup>

Owing to the fact that the  $\Upsilon(4S)$  can only decay to  $B\bar{B}$ , it is a relatively narrow resonance and prominent in the data. The  $\Upsilon(5S)$ , on the other hand, can decay to all nine ground state pseudoscalar and vector mesons and is relatively broad. In Fig. 6 its position is far from the real axis and relative to its width, its mass is near many sharp thresholds; the mass and width are 10.865 GeV and 110 MeV, respectively. Because of these complications, the  $\Upsilon(5S)$  does not have a normal Breit-Wigner shape and is hard to see in the cross sections. The  $\Upsilon(6S)$  mass is quoted in Ref. [13] as 11.019 GeV. We have included in Fig. 7 data only out to 10.99 GeV because we think that our calculated values in the region of the 6S are unreliable owing to the fact that we have not included channels with B mesons in excited states - either with  $\ell \neq 0$  or excited  $\ell = 0$  mesons; and these are likely to have thresholds in the vicinity of the  $\Upsilon(6S)$ .

The curves in Fig. 7 have been calculated without any adjustment of the parameters of the model. It is, therefore, in our opinion remarkable that they agree with the data as well as they do. As indicated at the end of section V, a mass shift matrix has been used to fix the

---

<sup>6</sup>We thank Dave Besson, Persis Drell and Elliot Chu for applying the radiative and beam spread corrections to the calculated cross sections.

peak values of the cross section at 10.580 GeV and 10.865 GeV. Aside from this, the energy dependence and the overall normalization of the calculated curves are determined by the models. The Zambetakis model (full curve) appears to fit the data around the  $\Upsilon(4S)$  better than the Cornell model (dashed curve). However, in the region of the  $\Upsilon(5S)$  the Cornell model may be a better fit.

As in the charm case, the energy dependence of the exclusive cross sections are quite different for the two models. The contributions to the cross section ratio R from the various channels are shown in Figs. 8 and 9; the full curves are for the  $B\bar{B}$  channels, neutral plus charged; the dot-dashed curves are for  $B\bar{B}^* + \bar{B}B^*$ ; and the dashed curves are for  $B^*\bar{B}^*$ . Notice that at the higher energies where these curves tend to flatten out they go over toward the proportion 1:4:7 which are the spin ratios, discussed in Ref. [2], for  $B\bar{B}$ ,  $B\bar{B}^* + \bar{B}B^*$ , and  $B^*\bar{B}^*$ , respectively. In Figs. 8 and 9 we omitted the  $\Upsilon(4S)$  resonance region because the cross section there is so much bigger than it is in the rest of the range.

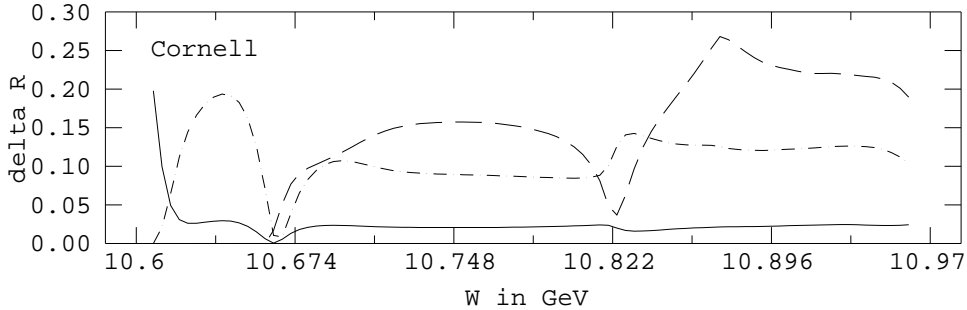


Figure 8.

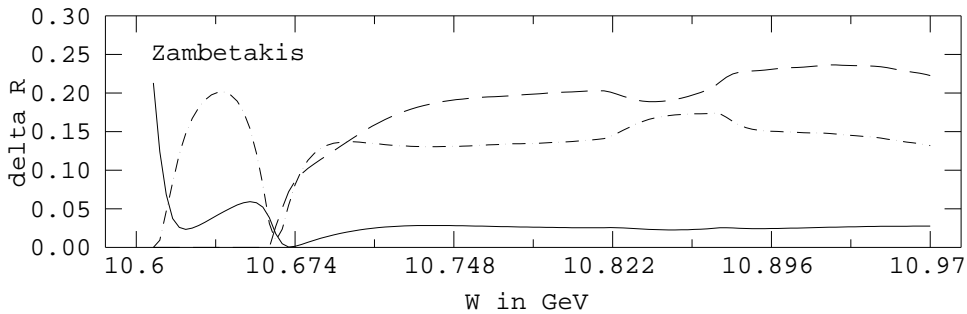
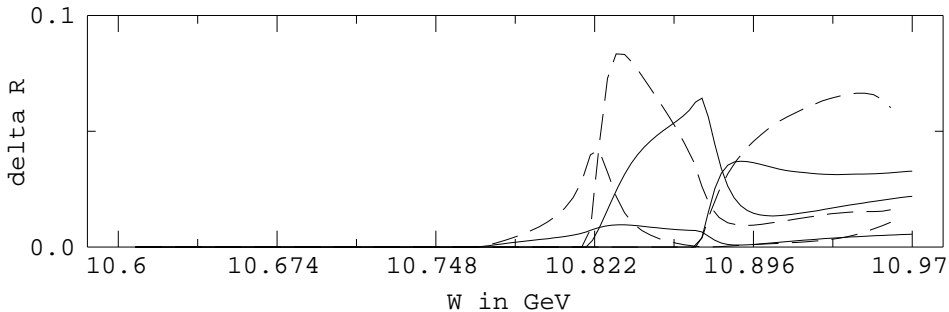


Figure 9.

Finally in Fig. 10 we show the contributions to  $R$  from  $B_s$  channels; the full curves are Cornell model predictions and dashed curves Zambetakis model. The curves for the various channels can be distinguished by their thresholds.



**Figure 10.**

One interesting feature of the curves in Fig. 10 is that both models predict relatively copious  $B_s\bar{B}_s^* + \bar{B}_s B_s^*$  production in the  $\Upsilon(5S)$  resonance region. (These predictions are sensitive to the  $B_s$  mass and the  $B_s^* - B_s$  mass difference.) As in the charm case, however, these models predict that the strange mesons are produced at a level of about 1/3 that of the nonstrange mesons. Note the change of scale in Fig. 10.

## VII. CONCLUSIONS

The fact that both the the Cornell and Zambetakis models, as simplistic as they are, can account very well for charmonium and  $\Upsilon$  narrow state spectroscopy and, without adjustment of parameters, give production cross sections which agree as well as they do with the data leads us to conclude that they merit further study. There are two directions for this. Experimentally, it would be interesting to compare calculated values for exclusive cross sections with measured values. From theoretical point of view, it may be worthwhile to evaluate taking predicted configuration mixing into account the allowed and forbidden M1 transition rates in charmonium and  $\Upsilon$  and compare those with measured values.

## ACKNOWLEDGMENTS

It is a pleasure to acknowledge the contributions to the computational side of this work from Stanley Cohen and staff of Speakeasy Corporation, and from the UCLA Office of Academic Computing. This work was supported in part by the Department of Energy grant FG03-91ER40662.



## REFERENCES

- [1] In this paper we will use  $Q$  for  $c$  or  $b$  and  $q$  for  $u$ ,  $d$ , or  $s$ .
- [2] E. Eichten, K. Gottfried, N. Kinoshita, K.D. Lane, and H.- M.Yan, Phys. Rev. D17, 3090 (1978); D21, 313(E)(1980); and Phys. Rev. D21, 203, (1980).
- [3] Estia Eichten and Frank Feinberg, Phys. Rev. D23, 2734 (1981).
- [4] Dieter Gromes, Z.Phys. C26, 401 (1984). See also Phys. Lett. 202B, 262 (1988).
- [5] V. Zambetakis, UCLA Ph.D. thesis (1985); available as UCLA research report UCLA/85/TEP/2.
- [6] H. Grotch, V.Zambetakis and N. Byers. (unpublished)
- [7] Richard Lee McClary, UCLA thesis (1982); N. Byers and R. L. McClary, Phys. Rev. D28, 1692(1983)
- [8] N. Brambilla and G. M. Prospero, Phys. Lett. B236,69 (1990).
- [9] T. Appelquist, R. M. Barnett, K. Lane in  $e^+e^-$  *Annihilation: New Quarks and Leptons*, Benjamin/Cummings pub., R. N. Cahn, ed..
- [10] V. A. Novikov et al., Phys. Rev. Lett. 38, 626 (1977) These authors pointed out that there is a  $(v/c)^2$  correction which gives direct coupling of the photon to  $^3D_1$  states. There is in addition a one gluon exchange correction to the quark-photon vertex which the Cornell group includes by multiplying the  $\ell = 0$  subspace of  $\mathcal{W}$  by  $(1 - 4\kappa/\pi)$ .
- [11] N. Byers and E. Eichten *Heavy Flavour Production near Threshold in  $e^+e^-$  Annihilation* (unpublished). N. Byers and E. Eichten, Nucl. Phys. B(Proc. Suppl.) 16, 281 (1990).
- [12] Le Yaouanc, L. Olivier, O. Pine, and J. C. Raynal, Phys, Rev. D 8, 2223 (1973); See also S. Ono, A. I. Sanda, and N. A. Tornqvist, Phys. Rev. D 35, 907 (1987) and references cited therein. Studies of B production in this model have also been made by Martin and Ng; cf., A. D. Martin and C.-K. Ng, preprint DTP/88/6. Fits to the production cross

sections are made with parameters in addition to those in the  $Q\bar{Q}$  potential and the quark pair creation strength  $\gamma_{QPC}$ .

[13] Particle Data Group, Phys. Rev. D50, 1177/(1994). The data points in Fig. 2 are those in that energy range in the graph on p.1334. We thank Michael Barnett and Tom Trippe for these selected data. The caption to this graph reads in part: “Systematic normalization errors are not included; they range from  $\sim 5\text{-}20\%$ , depending on experiment. We caution that especially the older experiments tend to have large normalization uncertainties.” Presumably BEPC will in future remeasure these cross sections.

[14] D. Z. Besson et al., Phys. Rev. Lett. 381 (1985). The constant non- $b\bar{b}$  background in R has been subtracted from these published data using the mean value 4.56 of the data points below beauty threshold, and the variance of these points has been added in quadrature with the published error to obtain the error bars in our graph.